Supporting Information (SI)

Coordinatively Unsaturated Structurally Diverse Homophthalate based Cobalt (II) Coordination Polymers for Efficient Multicomponent Catalysis

*Subham Sahoo[1], Rajesh Patra[1], and Debajit Sarma[1]**

[1]Department of Chemistry, Indian Institute of Technology Patna, Bihar 801106, India

*E-mail: debajit@iitp.ac.in

Contents

Materials and methods

All the solvents and reagents were purchased from commercial sources and used without further purification. The commercially obtained reagents mentioned above were used without further purification. The single crystal XRD diffraction data was collected using BRUKER AXS (D8 Quest System) X-ray diffractometer. Powder X-Ray diffraction patterns were recorded on PANalytical X'Pert Pro Diffractometer operated at 40 kV and 45 mA with Cu Kα radiation. The surface area measurement analysis was performed by the Quantachrome autosorb iQ2 analyzer. Thermogravimetric analysis was carried out using an SDT Q600 (TA Instruments), and the samples were heated from room temperature to 600°C at 10 °C min^{-1} rate under N_2 gas flow rate of 100 mL/min. ^1H NMR spectrum was recorded using a Bruker 400 MHz spectrometer. Energy calculations have been carried out by using the density function theory (DFT) exchange-correlation function B3LYP with basis set of 6-31+G**, to find out the optimized size of reactant and products.

Experimental section

Synthesis of [Co(4-ABPT)(HPA)(H_2O)], SSICG-8. A mixture of $Co(OAc)_2{\cdot}4H_2O$ (1 mmol), H_2HPA (1 mmol), and 4-ABPT (1 mmol) was taken in 5 mL of distilled water in a 10 mL glass vial. Then, the mixture was ultrasonicated for 10 min to make it homogeneous and heated to 150 °C for 3 days and then slowly cooled down to room temperature. Purple-colored, mixture of SSICG-8 were obtained, which were then filtered and thoroughly washed with water.

Synthesis of [Co(4-ABPT)(HPA) (H_2O)]·4H_2O, SSICG-9. A mixture of $Co(OAc)_2{\cdot}4H_2O$ (1 mmol), H_2HPA (1 mmol), and 4-ABPT (1 mmol) was taken in 5 mL of distilled water in a 10 mL glass vial. The mixture was ultrasonicated for 10 min to make it homogeneous and then heated at 90 °C for 10 minutes to make all the reactants soluble. After that, the temperature was cooled down to 30 °C. Purple-colored crystals of SSICG-9 was obtained after 3 days, which were then filtered and thoroughly washed with water.

Synthesis of [Co(BPY)(HPA)(H_2O)(CH_3OH)], SSICG-10. A mixture of $Co(OAc)_2 \cdot 4H_2O$ (1 mmol), H_2HPA (1 mmol), and 4,4'-bipyridine (BPY) (1 mmol) was taken in 5 mL of distilled water/methanol (1:1) in a 10 mL glass vial. Then, the mixture was stirred for 10 min to make it homogeneous and heated to 120 °C for 3 days and then slowly cooled down to room temperature. Purple-coloured, block-shaped X-ray quality crystals were obtained, which were then filtered and thoroughly washed with water.

Synthesis of [Co(4-ABPT)($HHPA)_2$]·H_2O, SSICG-16. A mixture of $Co(OAc)_2 \cdot 4H_2O$ (1 mmol), H_2HPA (2 mmol), and 4,4'-bipyridine (BPY) (1 mmol) was taken in 5 mL of distilled water/methanol (1:1) in a 10 mL glass vial. Then, the mixture was stirred for 10 min to make it homogeneous and heated to 120 °C for 3 days and then slowly cooled down to room temperature. Purple-coloured, block-shaped X-ray quality crystals were obtained, which were then filtered and thoroughly washed with water.

Heterogeneous catalysis

The catalytic reactions were studied using the following reaction procedure. After completion of a reaction, the reaction mixture was centrifuged to separate the catalyst and washed with ethanol. Column chromatography was performed to purify the products and yield calculation. The products were analyzed by ^1H NMR. Catalysts were dried within a desiccator for another cycle and PXRD.

Three-component Strecker reaction. Aldehyde (1 mmol), aniline (1 mmol), trimethylsilyl cyanide (TMSCN) (1 mmol), and catalyst (0.5 mol%) were taken in a 10 mL round bottom flask. After 1 h of vigorous stirring, following general procedure, the crude product was collected and purified.

Hantzsch condensation reaction. In a 10 mL round bottom flask, aldehyde (1 mmol), ammonium acetate (1 mmol), and ethyl acetoacetate (2 mmol), were dissolved in 1 mL of ethanol. After adding 1.5 mol% catalyst, the reaction was carried out at 60 °C for 4 h. Following the general procedure, the crude product was collected and purified.

Crystallographic data and structure refinements

Good quality single crystal of the compound was sorted out with the help of a polarizing microscope. The single crystal XRD diffraction data was collected using BRUKER AXS (D8 Quest System) X-ray diffractometer, equipped with a PHOTON 100 CMOS detector. The source of X-ray was a Mo Kα (λ = 0.71073 Å) radiation. Bruker Apex III software was used for data collection, unit cell measurements, absorption corrections, scaling, and integration.[1] The data were reduced, and an empirical absorption correction was applied with the help of SAINTPLUS and SADABS programs, respectively.[2-3] SHELXL97[4] present in the WinGx (Version 2023.1) programs was used to solve the crystal structures. The WinGx package of programs was used to carry out the full-matrix least-squares refinement against the function $|F^2|$.[5-7] The hydrogen atoms of the functional groups were fixed using the Olex2-1.5 package of programs.[6-7] 'OMIT' command has been used to remove bad reflections. The structure detail of the compound is presented in Table S1. CCDC: 2358730, 2358731, 2358732, and 2382838 contain the crystallographic data of these compounds. These data are available from The Cambridge Crystallographic Data Center (CCDC) *via* www.ccdc.cam.ac.uk/data_request/cif.

Table S1: Crystal data and structure refinement parameters for SSICG-8, SSICG-9, SSICG-10 and SSICG-16.

	SSICG-8	**SSICG-9**	**SSICG-10**	**SSICG-16**
Empirical formula	Co(4-ABPT)(HPA)(H_2O)	[Co(4-ABPT)(HPA)(H_2O)]·4H_2O	Co(BPY)(HPA)(H_2O)(CH_3OH)	[Co(4-ABPT)(HHPA)$_2$] ·H_2O
Formula weight	493.34	565.41	364.21	673.50
Wavelength(λ)	0.71073 Å	0.71073 Å	0.71073 Å	0.71073 Å
Crystal system	monoclinic	monoclinic	monoclinic	Triclinic
Space group	$P2_1/n$	$P2_1/c$	$P2_1/n$	$P\bar{1}$
a[Å]	8.644(2)	14.387(15)	13.245(6)	10.506(4)
b[Å]	8.559(2)	19.88(2)	8.885(4)	11.357(5)
c[Å]	27.039(7)	8.991(9)	14.381(6)	13.874(6)
α [°]	90.000	90.000	90.000	111.26(2)
β[°]	96.984(9)	105.436(4)	115.817(12)	105.15(2)
γ[°]	90.000	90.000	90.000	94.58(2)
Volume[Å^3]	1985.6(9)	2480.1(4)	1523.5(12)	1460.7(11)
Z	4	4	4	2
Density [Mg/m^3]	1.650	1.514	1.588	1.531
Abs. coeff. [mm^{-1}]	0.915	0.754	1.151	0.655
Abs. correction	None	None	None	None
F(000)	1012	1172	748	694
Reflections collected/ unique	43082 / 4975	42484 / 7486	18208 / 3996	35761 / 5071

R_{int}	0.0493	0.0842	0.0396	0.1409
Data / restraints / parameters	4975 / 0 / 304	7486 / 0 / 342	3996 / 0 / 210	5071 / 0 / 440
Min. 2θ/°	2.498	2.520	1.744	2.001
Max. 2θ/°	28.400	30.590	29.000	25.643
Ranges (h, k, l)	-11<=h<=11, -11<=k<=11, -36<=l<=36	-20<=h<=20, -28<=k<=28, -12<=l<=12	-17<=h<=15, -11<=k<=11, -19<=l<=19	-12<=h<=12, -13<=k<=13, -16<=l<=16
Complete to 2θ(%)	99.8	97.3	99.0	97.0
Refinement method	Full-matrix least-squares on F^2	Full-matrix least-squares on F^2	Full-matrix least-squares on F^2	Full-matrix least-squares on F^2
Goof (F^2)	1.138	1.040	1.165	1.069
Final R indices [$I>2\sigma(I)$]	R_1 = 0.0390, wR_2=0.0744	R_1 = 0.0557, wR_2= 0.1221	R_1 = 0.0529, wR_2= 0.0948	R_1 = 0.0951, wR_2 = 0.1829
R indices (all data)	R_1 = 0.0522, wR_2=0.0808	R_1 = 0.1083, wR_2= 0.1553	R_1 = 0.0691, wR_2= 0.1019	R_1 = 0.1759, wR_2 = 0.2315
CCDC No.	**2358730**	**2358731**	**2358732**	**2382838**

Structural analysis

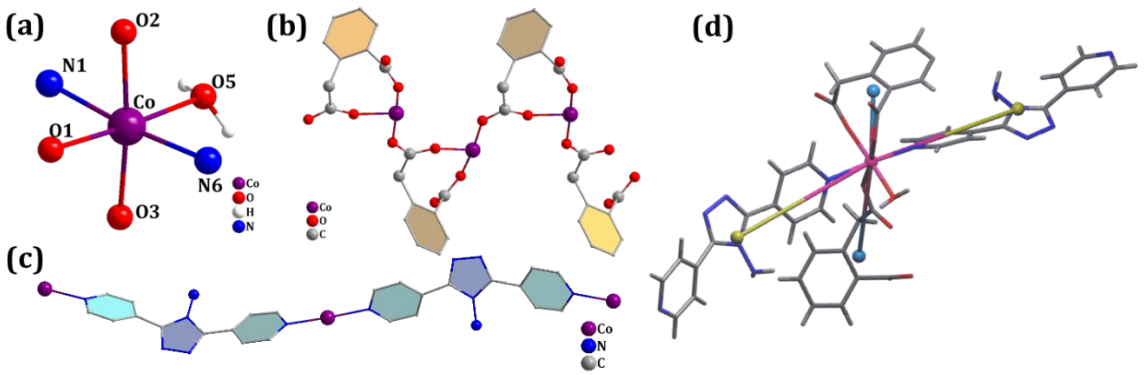

Figure S1. (a) Coordination environment of Co; binding motif of (b) HPA, (c) 4-ABPT; (d) topological representation of SSICG-8.

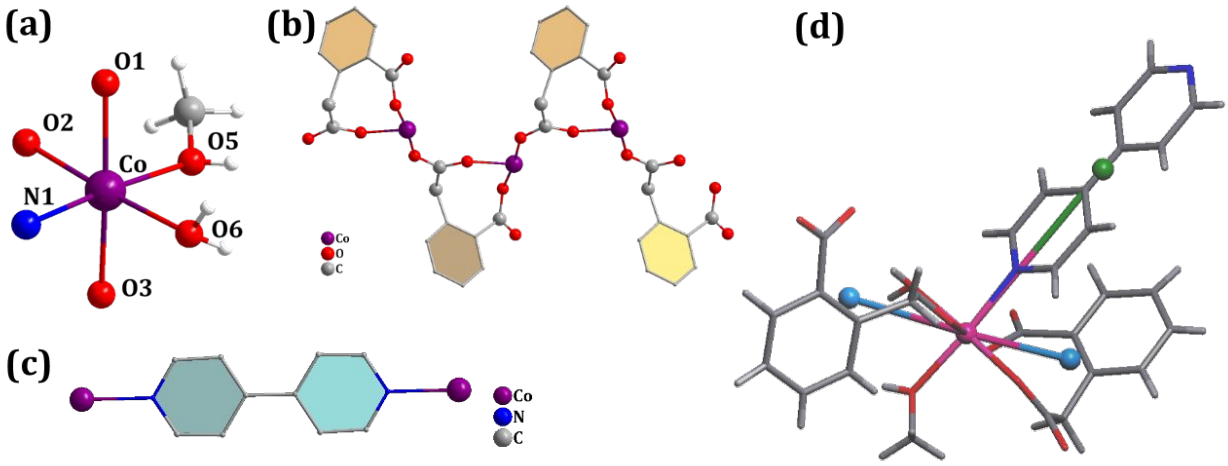

Figure S2. (a) Coordination environment of Co; binding motif of (b) HPA, (c) BPY; (d) topological representation of SSICG-10.

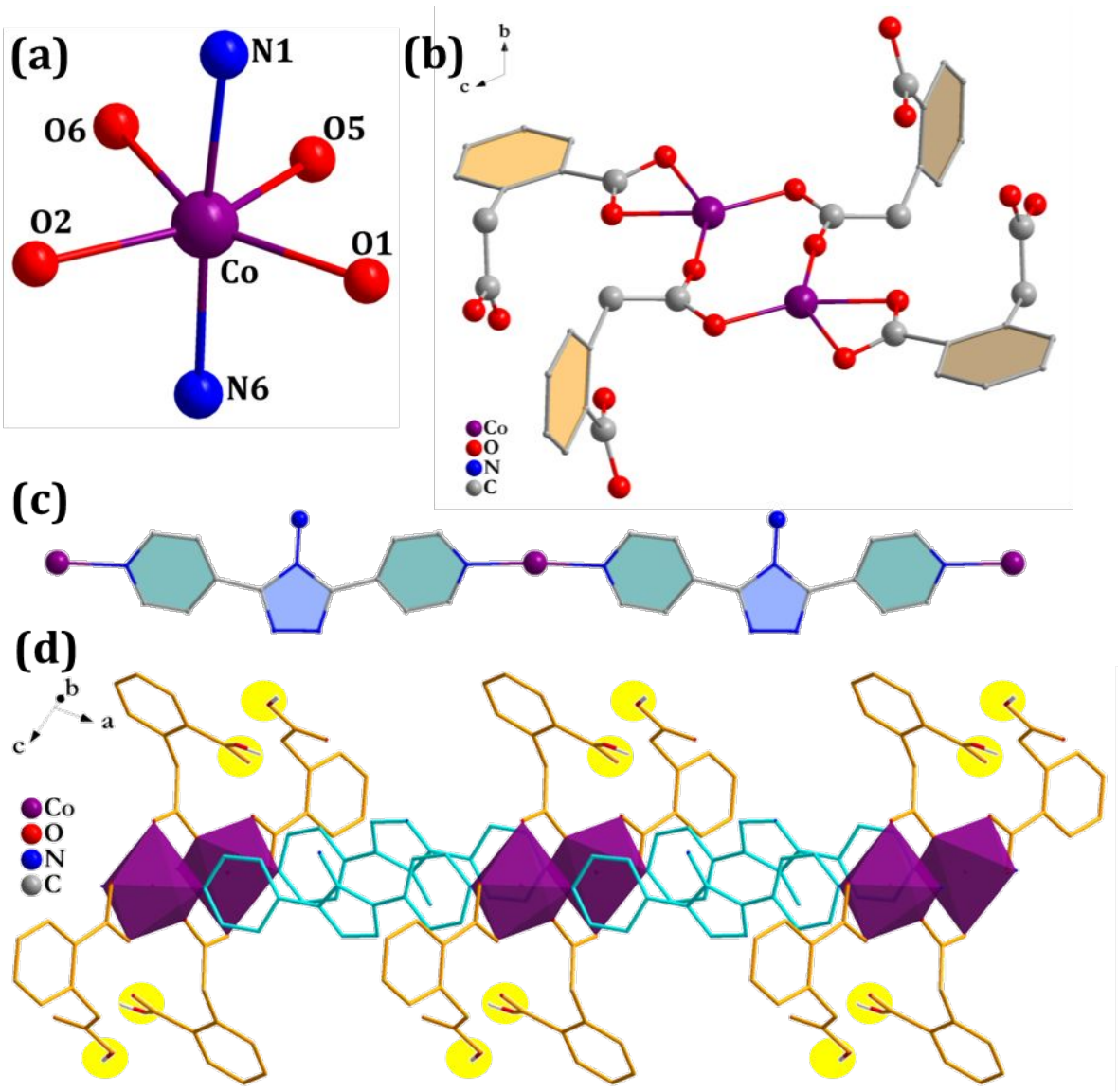

Figure S3. (a) Coordination environment of Co; binding motif of (b) HPA, (c) 4-ABPT; (d) 1D chain of SSICG-16 (protonated carboxylic acid groups of homophthalic acids are highlighted).

Characterization

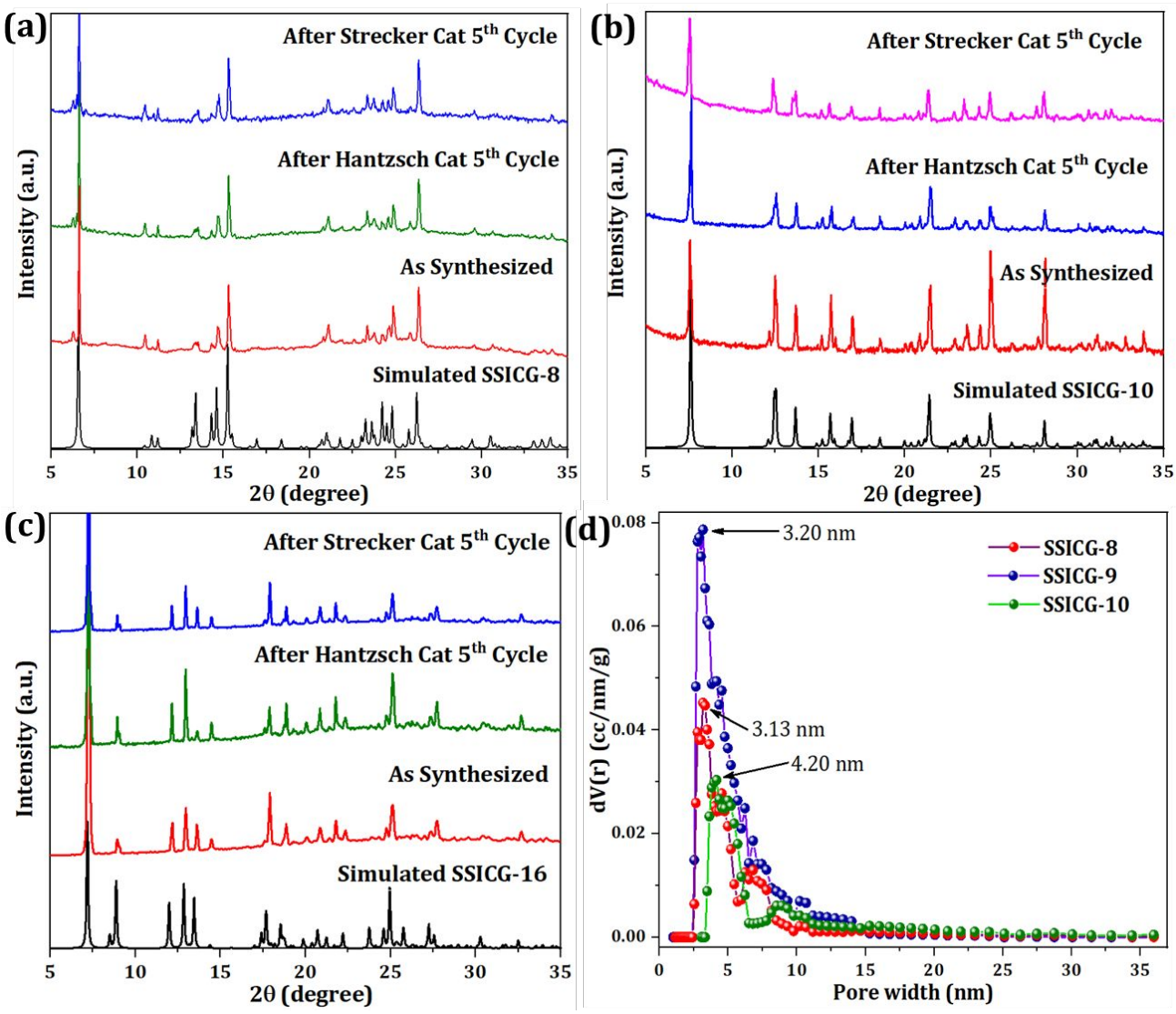

Figure S4. PXRD patterns of (a) SSICG-8, (b) SSICG-9, (c) SSICG-16 and (d) pore size distribution of SSICG-8, SSICG-9 and SSICG-10.

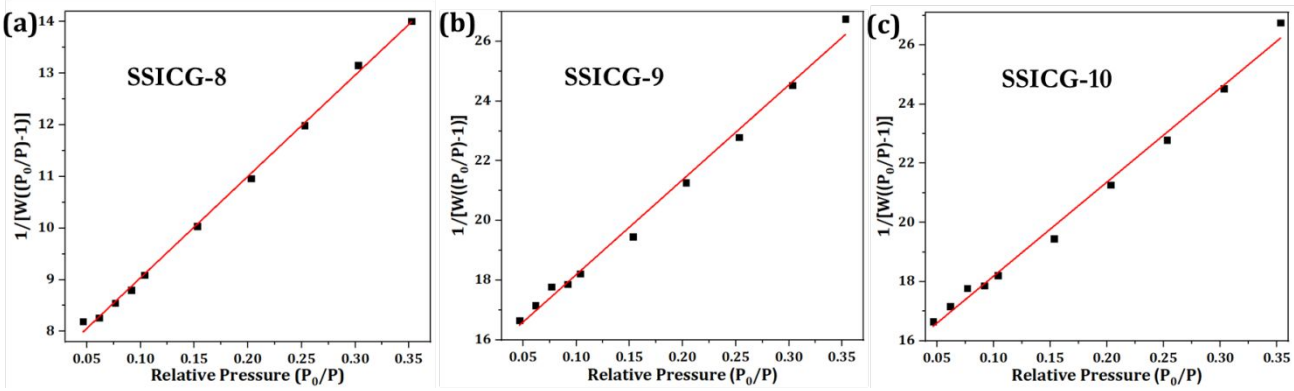

Figure S5. Multipoint BET plot of SSICG-8, SSICG-9 and SSICG-10.

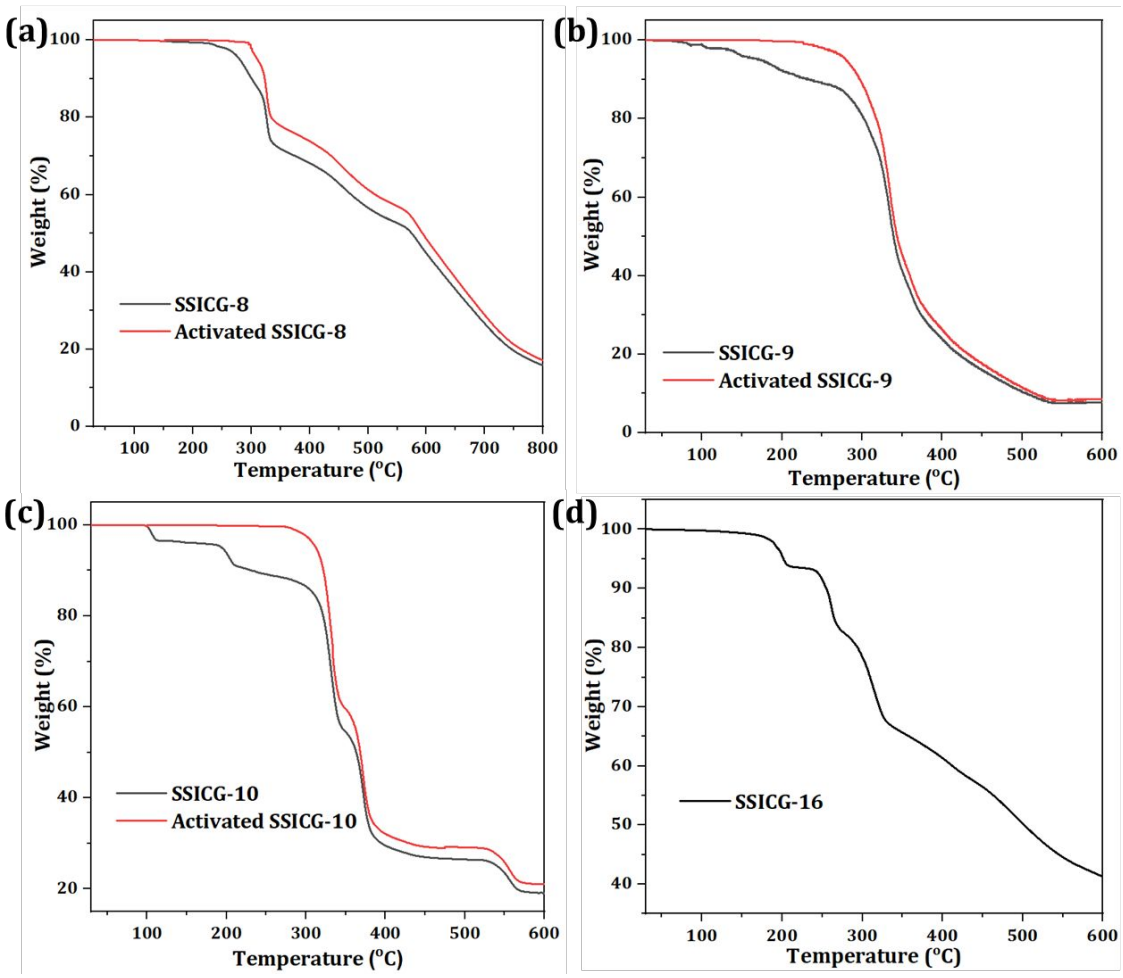

Figure S6. TGA plot of SSICG-8, SSICG-9, SSICG-10 and SSICG-16.

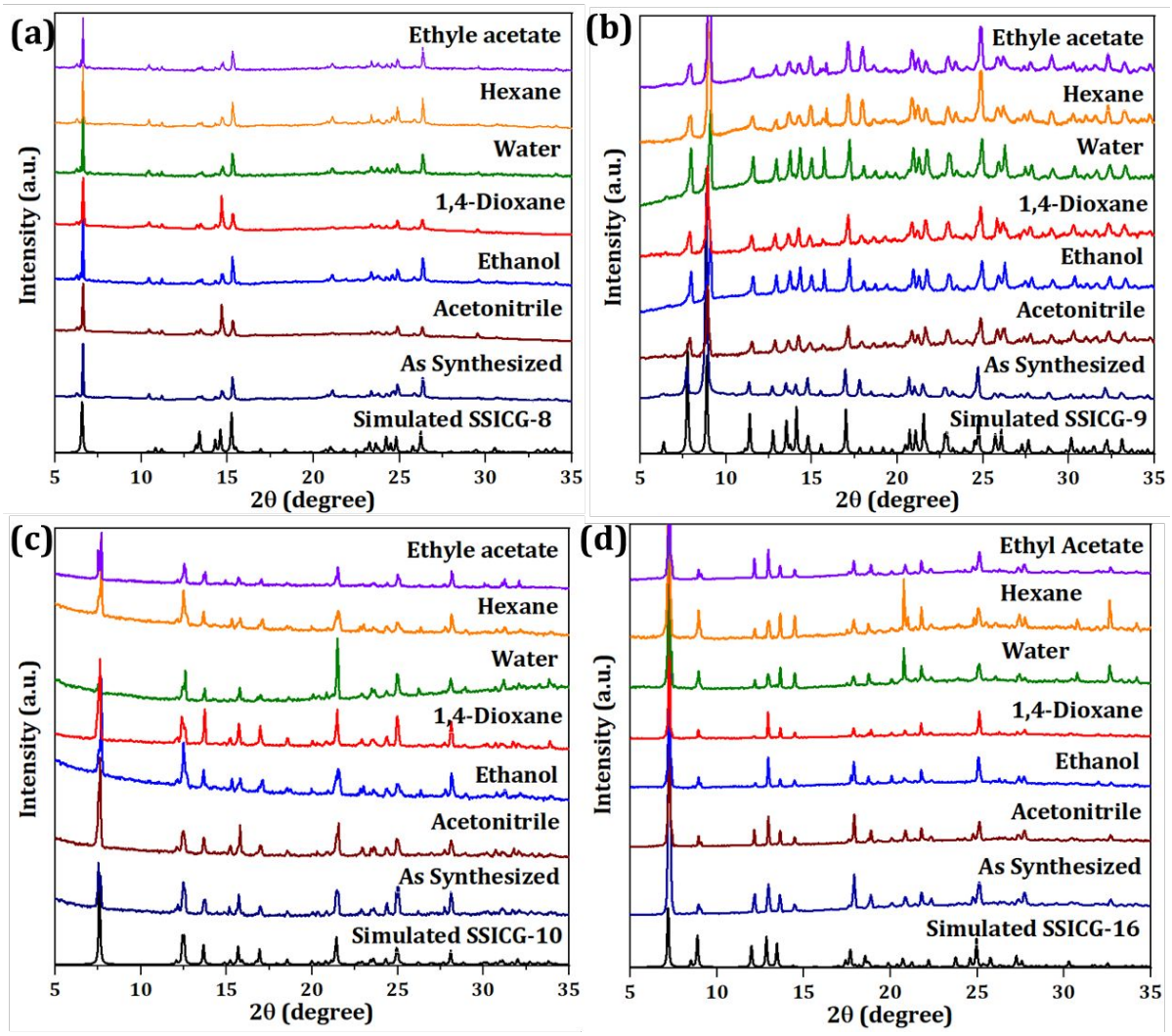

Figure S7. PXRD patterns after boiling SSICG-8, SSICG-9, SSICG-10 and SSICG-16 in conventional solvents for six hours.

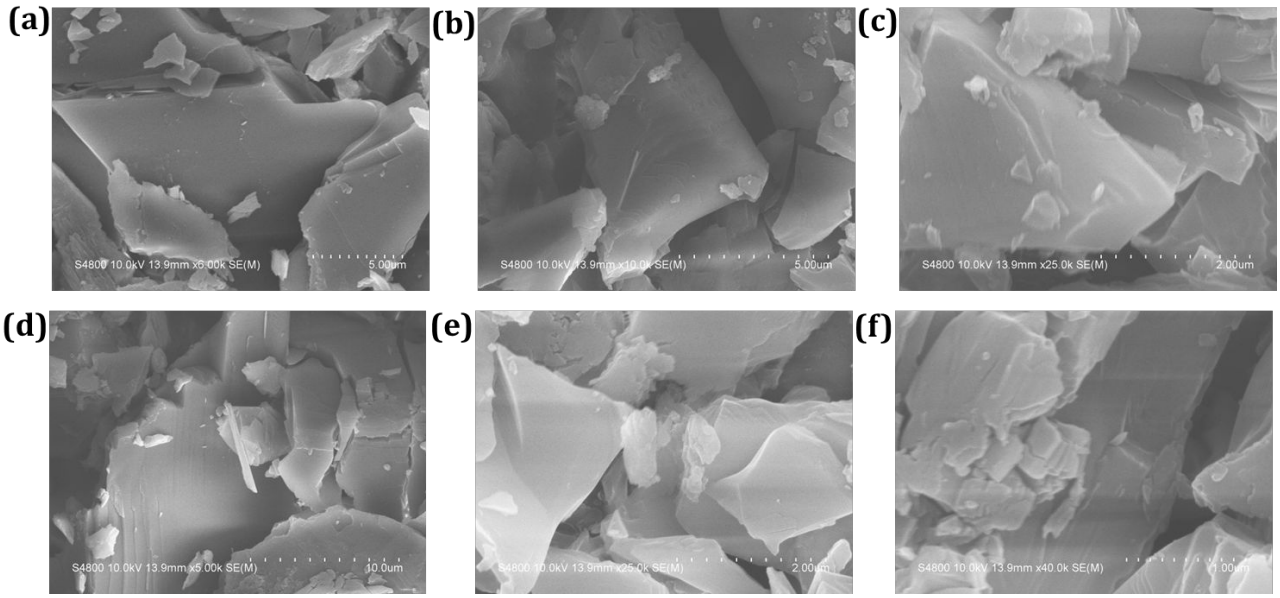

Figure S8. SEM images of (a) SSICG-9; after boiling in conventional solvents including (b) acetonitrile, (c) ethanol, (d) 1,4-dioxane, (e) water, (f) hexane for six hours.

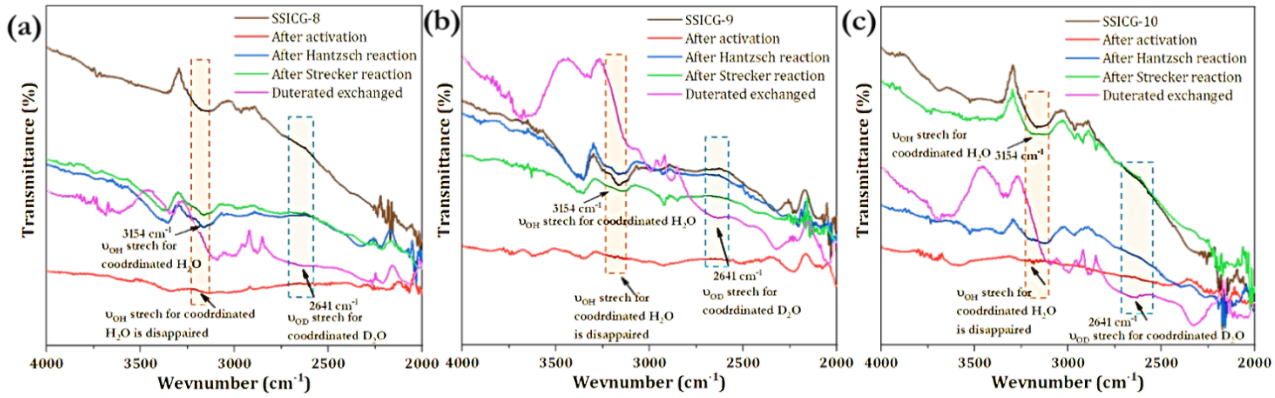

Figure S9. IR spectra of SSICG-8, SSICG-9 and SSICG-10 after activation, after catalysis and deuterated exchanges.

Three component Strecker reaction

Table S2. Controlled reaction data for the Strecker reactions[a]

Entry	Catalyst	Temperature (°C)	Time (h)	Yield[b] (%)
1	$Co(OAc)_2{\cdot}4H_2O$	rt	1	24
3	H_2HPA			17
4	4-ABPT			-
5	$Co(OAc)_2{\cdot}4H_2O$ + H_2HPA + 4-ABPT			23
6	-			-
7	SSICG-16			38
8	SSICG-10			76
9	SSICG-8			84
10	SSICG-9			96

[a]Reaction condition: benzaldehyde (1 mmol), aniline (1 mmol), TMSCN (1.1 mmol), 0.5 mol% of SSICG-9 used as a catalyst, solvent-free, rt.
[b]Isolated yields based on aldehyde.

Table S3. Comparison table of CPs/MOFs used as heterogeneous catalysts for three-component Strecker reaction under solvent-free conditions.

Entry	Catalyst	mol%	Temp (°C)	Time (h)	Yield (%)	Ref.
1	$[Zn_2(hipamifba)_2(H_2O)_2]{\cdot}4H_2O$	2	25	6	79	8
2	$[Cd_2(hipamifba)_2(H_2O)_4]{\cdot}8H_2O$	2	25	6	100	
3	$In_3O(btb)_2(HCOO)L$	0.5	25	3.5	99	9
4	$In_{36}(\mu\text{-}OH)_{24}(NO_3)_8(Imtb)_{24}$	0.1	25	3	99	10
5	$In_3O(pbpta)_{1.5}(H_2O)_3$	0.88	25	0.5	99	11
6	$Cd_2(L)(H_2O)(DMF)]{\cdot}3DMF{\cdot}2H_2O$	1	25	4	99	12
7	$[Cd(bpp)(L)(H_2O)]{\cdot}DMF$	3	30	6	91	13
8	$[Zn_2(3\text{-}tpom)(L)_2]{\cdot}2H_2O$	1	25	5	90	14
9	$[(CH_3)_2NH_2][Zn_2(L)(H_2O)(PO_4)]{\cdot}2DMF$	2.4	25	0.5	99	15
10	$[Cd_4(L1)_4(DMF)_6]_n{\cdot}3n(DMF)$	1	80	4	96	16
11	$[In_{0.72}Ga_{0.28}(O_2C_2H_4)_{0.5}(hfipbb)]$	1	rt	96	64	17
12	$[In_{0.55}Ga_{0.45}(O_2C_2H_4)_{0.5}(hfipbb)]$	1	rt	1.33	91	17
13	$[Co_2(\mu_2\text{-}O)(TDC)_2(L)(H_2O)_2]{\cdot}2DMF$	0.3	25	1	100	18

14	$[Cd(hipamifba)(H_2O)_2]\cdot 2H_2O$	2	25	6	100	[19]
15	$[Zn(hipamifba)(H_2O)]\cdot 2H_2O$	2	25	6	79	[19]
16	$[Zn_4(\mu_3\text{-}OH)_2(d\text{-}2,4\text{-}cbs)_2(H_2O)_4].5H_2O$	5	40	5	92	[20]
17	$[In_3(NIPH)_3(HNIPH)(OH)_2]\cdot 4H_2O$	9.6	rt	24	96	[21]
18	$[Bi_{14}(\mu_3\text{-}O)_9(\mu_4\text{-}O)_2(\mu_3\text{–}OH)_5$ (3,5-DSB)$_5(H_2O)_3]\cdot 7H_2O$	1	rt	4	95	[22]
19	**SSICG-16**	**0.5**	**25**	**1**	**38**	**This work**
20	**SSICG-10**	**0.5**	**25**	**1**	**76**	
21	**SSICG-8**	**0.5**	**25**	**1**	**84**	
22	**SSICG-9**	**0.5**	**25**	**1**	**96**	

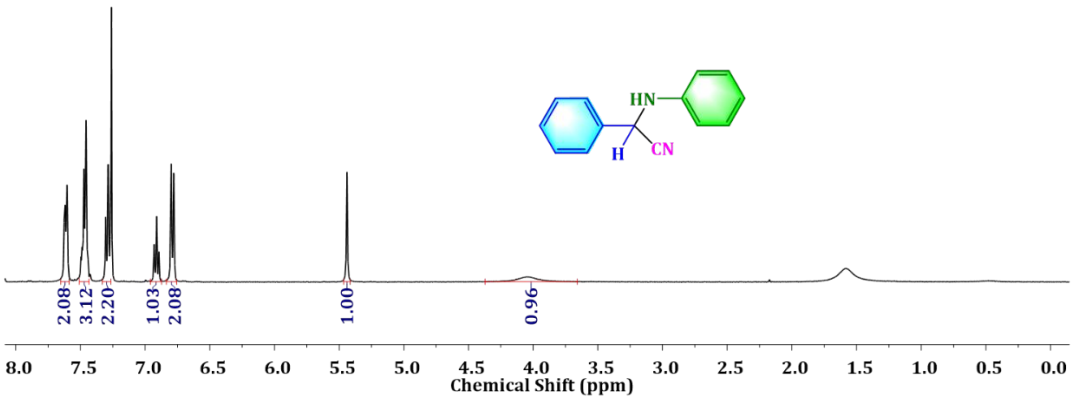

Figure S10. ^{1}H NMR spectra for 1a.

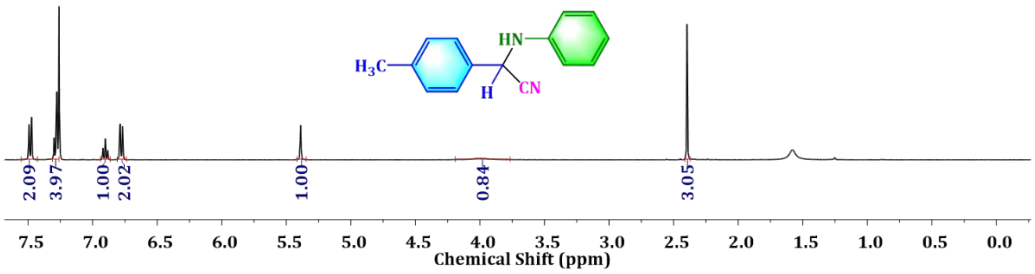

Figure S11. ^{1}H NMR spectra for 1b.

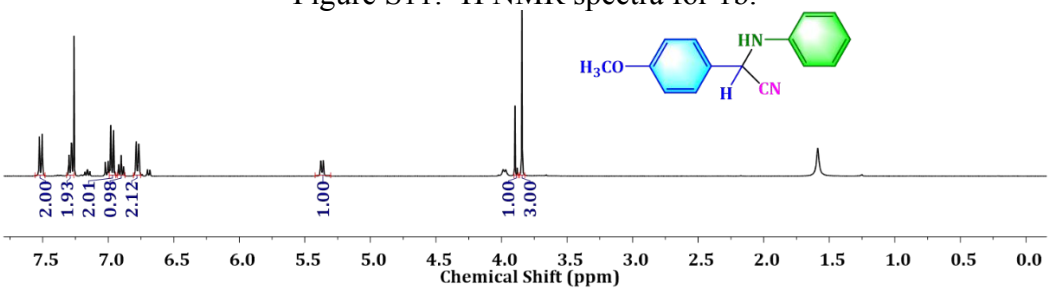

Figure S12. ^{1}H NMR spectra for 1c.

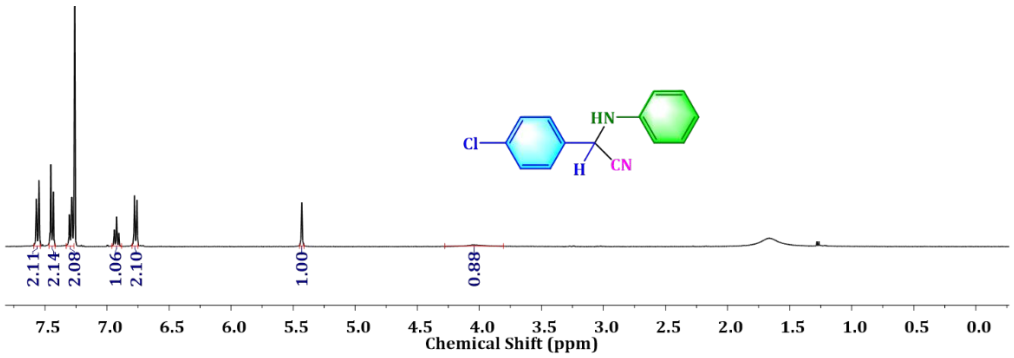

Figure S13. ^{1}H NMR spectra for 1d.

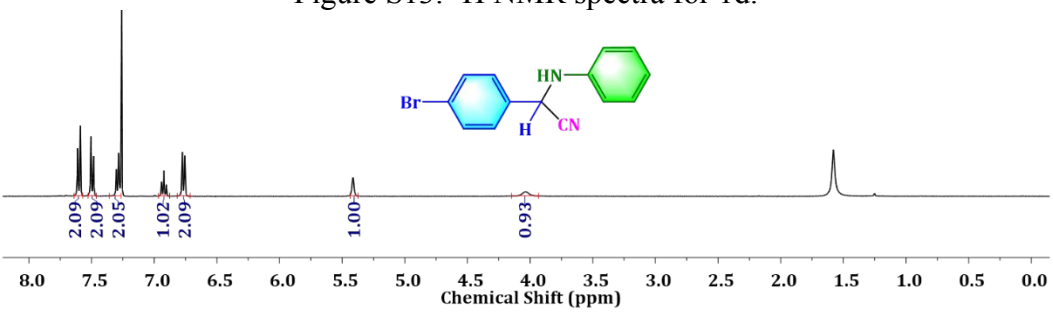

Figure S14. ^{1}H NMR spectra for 1e.

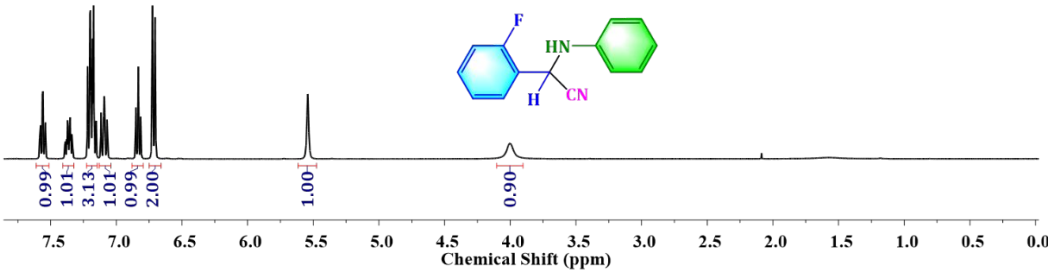

Figure S15. ^{1}H NMR spectra for 1f.

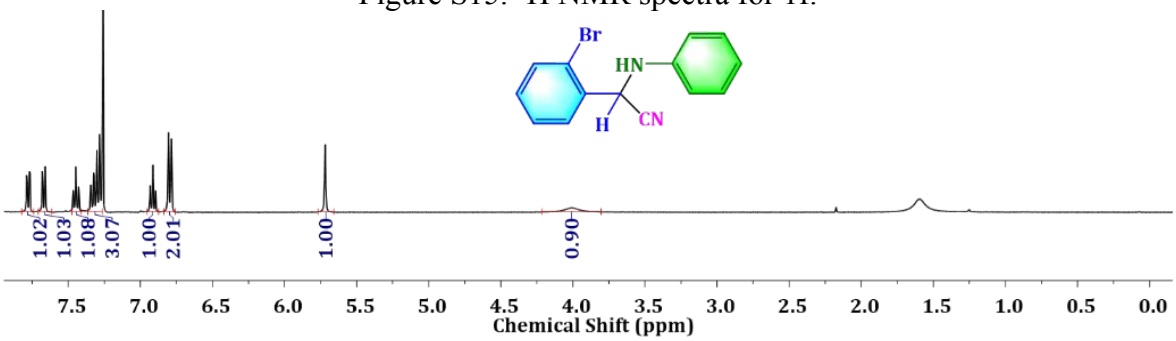

Figure S16. ^{1}H NMR spectra for 1g.

Hantzsch condensation reaction

Table S4. Optimization table for Hantzsch condensation reaction[a]

Entry	Solvent	Cat. SSICG-9 (mol%)	Time (h)	Temperature (°C)	Yield[b] (%)
1	-	1.5	4	60	13
2	H_2O				22
3	MeOH				54
4	EtOH				**95**
5			3		76

6			1.5		64
8		1.0	4		86
9		0.5		60	79
10		1.5		50	71
11				40	53

[a]Reaction condition: benzaldehyde (1 mmol), ammonium acetate (1 mmol), ethyl acetoacetate (2 mmol), SSICG-9 used as a catalyst.
[b]Isolated yields based on aldehyde.

Table S5. Controlled reaction data for the Hantzsch condensation reactions[a]

Entry	Catalyst	Solvent	Temp. (°C)	Time (h)	Yield[b] (%)
1	$Co(OAc)_2 \cdot 4H_2O$	EtOH	60	4	26
3	H_2HPA				19
4	4-ABPT				-
5	$Co(OAc)_2 \cdot 4H_2O$ + H_2HPA + 4-ABPT				29
6[b]	SSICG-9				48
7	-				-
8	SSICG-16				35
9	SSICG-10				78
10	SSICG-8				81

[a]Reaction condition: benzaldehyde (1 mmol), ethyl acetoacetate (2 mmol), ammonium acetate (1 mmol), solvent (1 mL), catalyst (1.5 mol %). [b]Isolated yields based on aldehyde.
[b]Catalyst was removed after 30 min

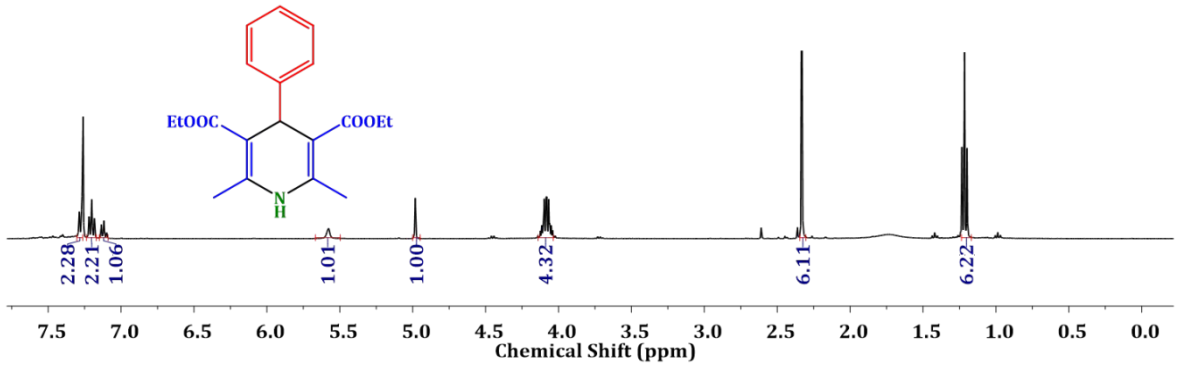

Figure S17. ^{1}H NMR spectra for 2a.

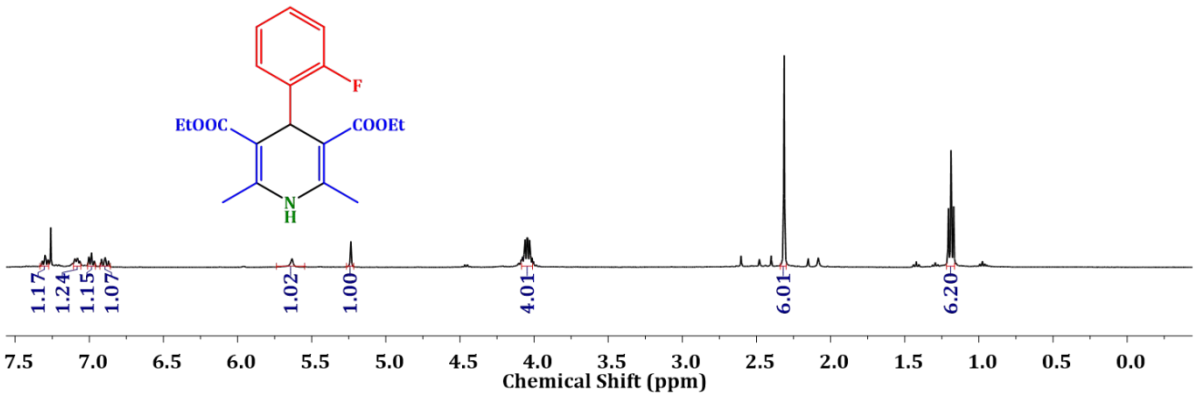

Figure S18. ^{1}H NMR spectra for 2b.

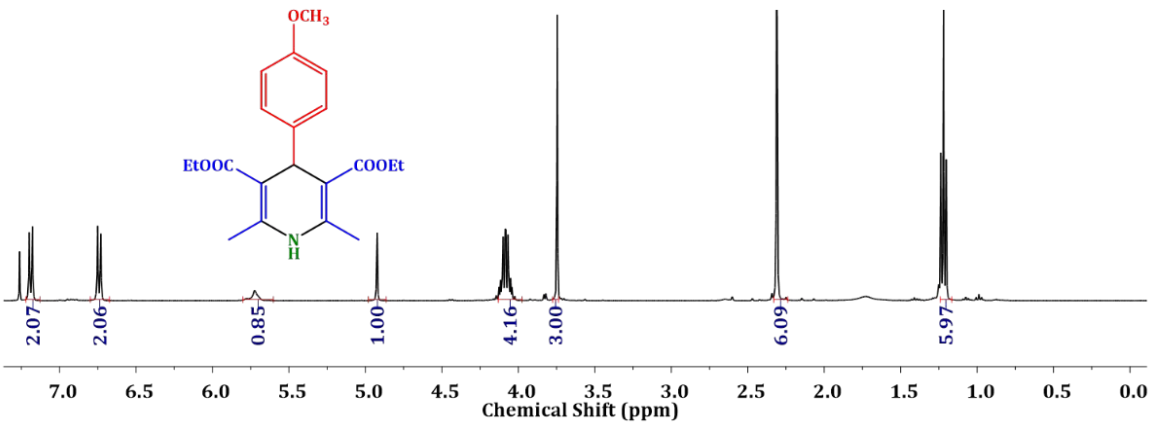

Figure S19. ^{1}H NMR spectra for 2c.

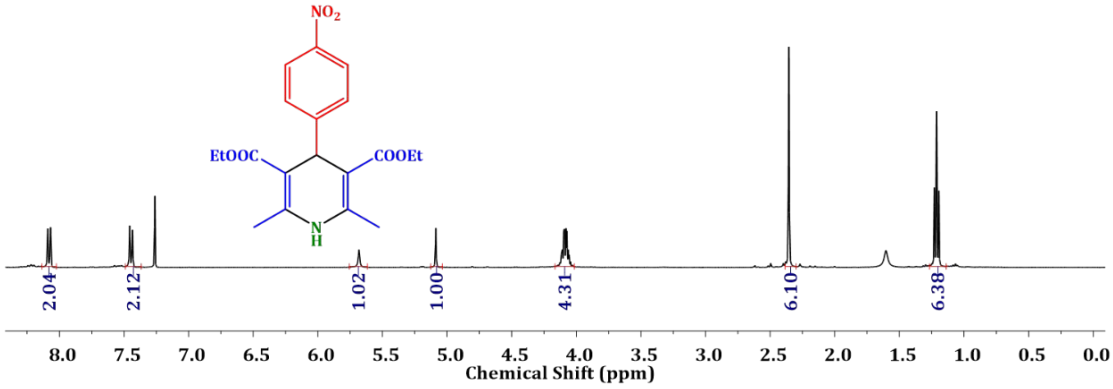

Figure S20. ^{1}H NMR spectra for 2d.

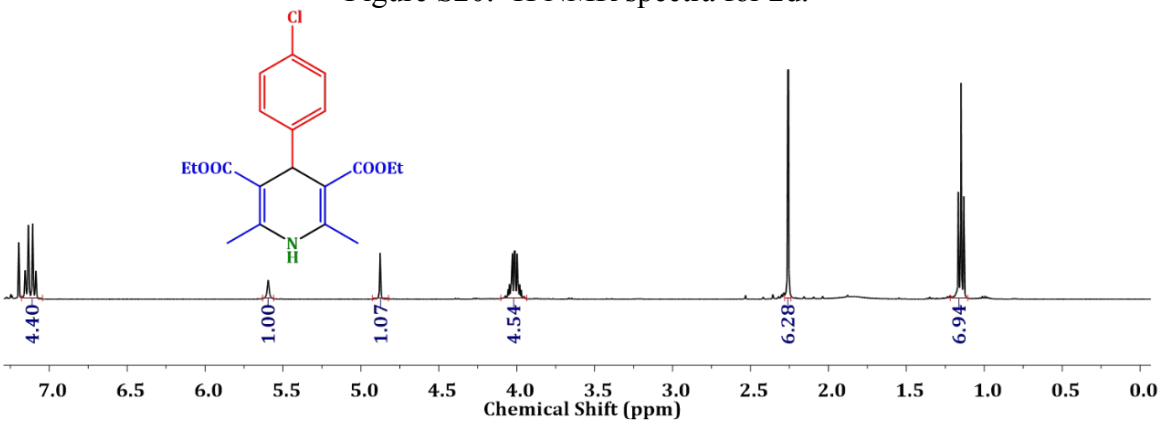

Figure S21. ^{1}H NMR spectra for 2e.

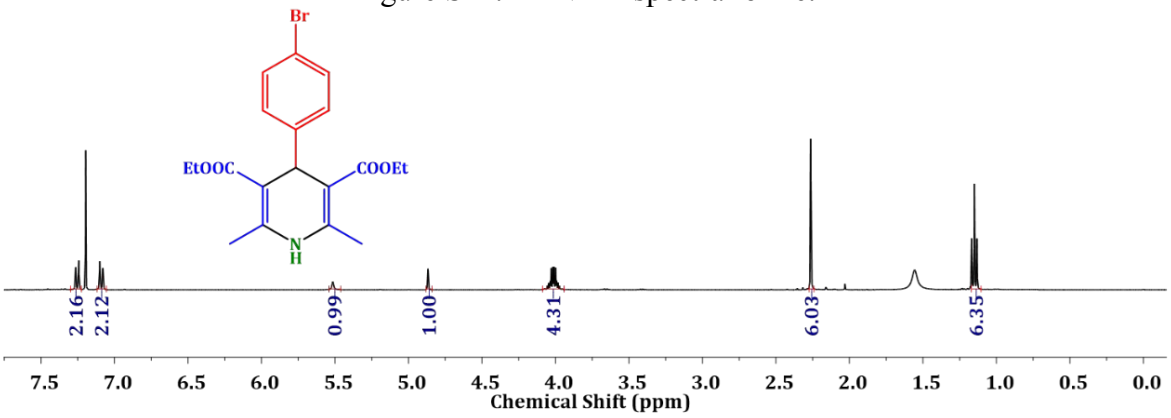

Figure S22. ^{1}H NMR spectra for 2f.

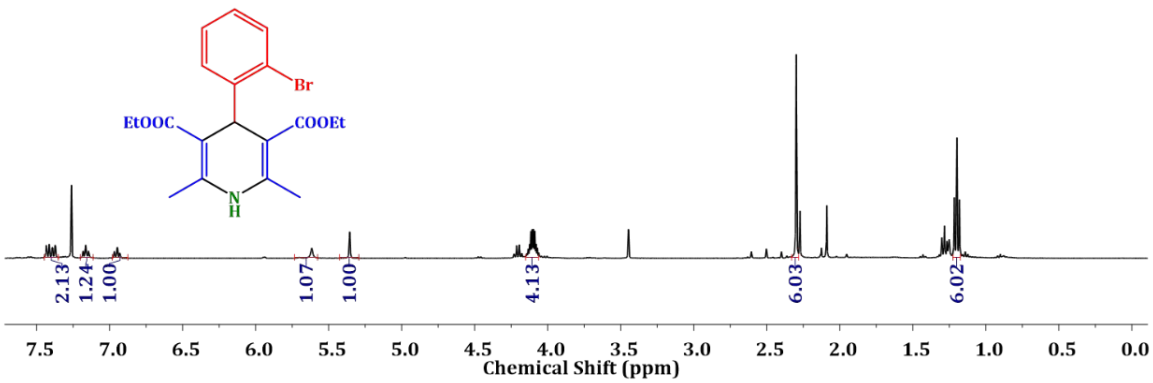

Figure S23. ^{1}H NMR spectra for 2g.

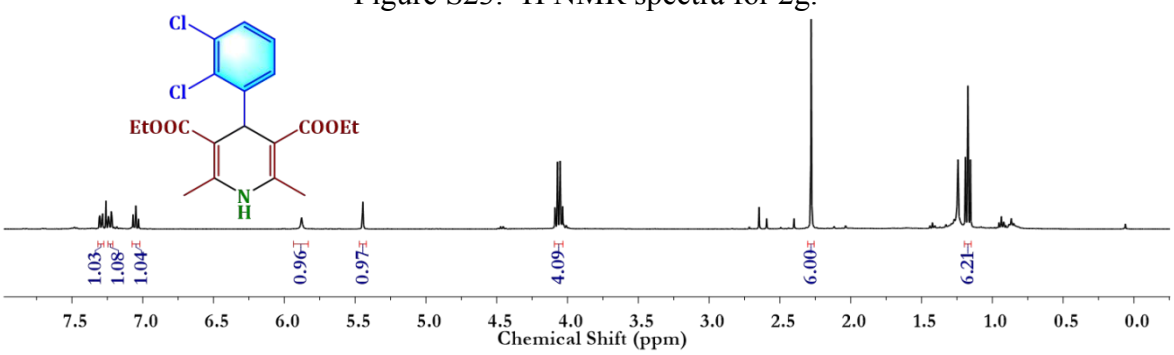

Figure S24. ^{1}H NMR spectra for Nemadipine B drug molecule.

Table S6. Comparison table for the catalytic Hantzsch condensation performance of with other reported heterogeneous catalysts.

Entry	Catalyst	Temp (°C)	Time (h)	Yield (%)	Ref.
1	TMU-33	rt	2	96	23
2	Fe-TUD-1	80	5	76	24
3	Zr-SBA-16	80	3	77	25
4	IR-MOF-3	reflux	5	89	26
5	Cu(II)-MOF	60	2	98	27
6	$Dy(DBM)_3$.bpy	80	5	93	28
7	$Cd(H_4L)_{0.5}(4,4';\text{-bpy})_{0.5}(H_2O)_2$	60	4	99	29
8	MIL-101(Cr)	80	2	98	30
9	$FeAl_2O_4$	100	3	90	31
10	Fe_3O_4-TEDETA-Br_3	80	2	92	32
11	$Cu(L1)(H_2O)_2$	90	2	98	33
12	Er(III)-MOF	70	4	85	34
13	MIL-101-SO_3H	60	8	99	35
14	Mn-MOF	80	0.5	98	36
15	**SSICG-16**	**60**	**4**	**35**	**This work**
16	**SSICG-10**	**60**	**4**	**78**	
17	**SSICG-8**	**60**	**4**	**81**	
18	**SSICG-9**	**60**	**4**	**95**	

Table S7. Selected bond distances (Å) and bond angles (°).

SSICG-8

Co-O(1)	2.0583(16)	Co-O(5)	2.0837(16)	Co-N(6)#2	2.1619(17)
Co-O(3)	2.0770(16)	Co-O(2)#1	2.1045(15)	Co-N(1)	2.1695(17)

O(1)-Co-O(3)	97.17(6)	O(5)-Co-N(6)#2	88.23(6)
O(1)-Co-O(5)	176.90(7)	O(2)#1-Co-N(6)#2	88.85(6)
O(3)-Co-O(5)	85.81(7)	O(1)-Co-N(1)	89.99(7)
O(1)-Co-O(2)#1	80.66(6)	O(3)-Co-N(1)	87.09(6)
O(3)-Co-O(2)#1	174.04(6)	O(5)-Co-N(1)	89.28(6)
O(5)-Co-O(2)#1	96.30(6)	O(2)#1-Co-N(1)	87.37(6)
O(1)-Co-N(6)#2	92.28(7)	N(6)#2-Co-N(1)	175.22(7)
O(3)-Co-N(6)#2	96.80(6)		

Symmetry transformations used to generate equivalent atoms. #1 -x+1/2,y+1/2,-z+3/2; #2 x-1/2,-y+3/2,z+1/2

SSICG-9

Co(1)-O(1)	2.070(2)	Co(1)-O(5)	2.085(2)	Co(1)-N(1)	2.169(2)
Co(1)-O(3)	2.081(2)	Co(1)-O(4)#1	2.125(2)	Co(1)-N(6)#2	2.188(2)

O(1)-Co(1)-O(3)	97.45(9)	O(5)-Co(1)-N(1)	87.99(9)
O(1)-Co(1)-O(5)	87.50(10)	O(4)#1-Co(1)-N(1)	85.19(8)
O(3)-Co(1)-O(5)	174.98(9)	O(1)-Co(1)-N(6)#2	87.89(9)
O(1)-Co(1)-O(4)#1	177.49(8)	O(3)-Co(1)-N(6)#2	85.76(9)
O(3)-Co(1)-O(4)#1	83.08(8)	O(5)-Co(1)-N(6)#2	95.30(9)
O(5)-Co(1)-O(4)#1	92.01(9)	O(4)#1-Co(1)-N(6)#2	89.70(8)
O(1)-Co(1)-N(1)	97.24(9)	N(1)-Co(1)-N(6)#2	174.03(10)
O(3)-Co(1)-N(1)	90.55(9)		

Symmetry transformations used to generate equivalent atoms. #1 x,-y+1/2,z+1/2; #2 x-1,y,z-1.

SSICG-10

Co(1)-O(1)	2.069(2)	Co(1)-O(3)	2.095(2)	Co(1)-N(1)	2.145(2)
Co(1)-O(2)#1	2.088(2)	Co(1)-O(5)	2.096(2)	Co(1)-O(6)	2.149(2)

O(1)-Co(1)-O(2)#1	80.41(8)	O(3)-Co(1)-N(1)	92.12(9)
O(1)-Co(1)-O(3)	95.02(8)	O(5)-Co(1)-N(1)	88.03(8)
O(2)#1-Co(1)-O(3)	174.83(8)	O(1)-Co(1)-O(6)	91.39(9)
O(1)-Co(1)-O(5)	176.26(8)	O(2)#1-Co(1)-O(6)	90.59(10)
O(2)#1-Co(1)-O(5)	96.53(8)	O(3)-Co(1)-O(6)	87.09(9)
O(3)-Co(1)-O(5)	87.95(8)	O(5)-Co(1)-O(6)	86.49(8)
O(1)-Co(1)-N(1)	94.12(9)	N(1)-Co(1)-O(6)	174.49(9)
O(2)#1-Co(1)-N(1)	90.62(9)		

Symmetry transformations used to generate equivalent atoms. #1 -x+3/2,y+1/2,-z+1/2; #2 -x+1,-y+1,-z+1.

SSICG-16

Co(1)-O(1)	2.070(6)	Co(1)-N(1)	2.140(5)	Co(1)-O(5)	2.160(6)
Co(1)-O(2)#1	2.096(5)	Co(1)-N(6)#2	2.152(6)	Co(1)-O(6)	2.264(5)

O(1)-Co(1)-O(2)#1	122.0(2)	N(1)-Co(1)-O(5)	91.8(2)
O(1)-Co(1)-N(1)	88.3(2)	N(6)#2-Co(1)-O(5)	84.9(2)
O(2)#1-Co(1)-N(1)	93.7(2)	O(1)-Co(1)-O(6)	146.0(2)
O(1)-Co(1)-N(6)#2	88.9(2)	O(2)#1-Co(1)-O(6)	92.00(19)
O(2)#1-Co(1)-N(6)#2	90.3(2)	N(1)-Co(1)-O(6)	90.1(2)
N(1)-Co(1)-N(6)#2	175.8(2)	N(6)#2-Co(1)-O(6)	90.5(2)
O(1)-Co(1)-O(5)	87.0(2)	O(5)-Co(1)-O(6)	59.11(19)
O(2)#1-Co(1)-O(5)	150.6(2)		

Symmetry transformations used to generate equivalent atoms. #1 -x+1,-y+2,-z+2 #2 x+1,y+1,z.

Table S8. H-bonding interactions

SSICG-8

D --H …A	d(H…A) (Å)	D(D…A) (Å)	< DHA (^{O})
O5 --H5A ..O4#1	1.96	2.760(2)	157
O5 --H5C ..O2#2	2.02	2.806(2)	154
O5 --H5C ..O1#3	2.31	2.916(2)	128

Symmetry transformations used to generate equivalent atoms. #1 1/2-x,-1/2+y,1/2-z; #2 x,-1+y, z ; #3 3/2-x,-1/2+y,1/2-z

SSICG-9

D --H …A	d(H…A) (Å)	D(D…A) (Å)	< DHA (^{O})
O5 --H5A ..O4#1	2.41	3.075 (3)	134
O5 --H5A ..O3#2	2.01	2.787(3)	148
O5 --H5B ..O100#3	1.99	2.676(4)	135
N5 --H5D ..N2#2	2.36	3.074(4)	141
N5 --H5E ..O2#4	2.00	2.872(4)	172
O103 --H10B ..O1#1	2.18	3.153(4)	173
O103 --H10B ..O2#1	2.52	3.227(4)	130
O101 --H10C ..O2#5	2.13	2.839(4)	141

Symmetry transformations used to generate equivalent atoms. #1 x,y,1+z; #2 x,1/2-y,1/2+z; #3 -x,-1/2+y,3/2-z; #4 1-x,-y,2-z; #5 x,1/2-y,-1/2+z

SSICG-10

D --H …A	d(H…A) (Å)	D(D…A) (Å)	< DHA (^{O})
O5 --H5A ..O3#1	2.05	2.755(3)	138
O5 --H5B ..O2#2	2.23	3.074(3)	165
O5 --H5B ..O1#3	2.37	2.824(3)	113

Symmetry transformations used to generate equivalent atoms. #1 1-x, 1-y, -z; #2 x,1+y, z; #3 3/2-x,1/2+y,1/2-z.

SSICG-16

D --H …A	d(H…A) (Å)	D(D…A) (Å)	< DHA (°)
O4 --H4 ..O100#1	1.87	2.673(10)	167
N5 --H5A ..O6#2	2.18	3.017(10)	139
N5 --H5B ..O2#3	2.18	2.817(10)	134
O7 --H7 ..O8#4	2.01	2.817(11)	169
O100 --H10B ..N3#5	2.02	2.870(9)	177
O100 --H10C ..O6#6	2.15	2.967(9)	160

Symmetry transformations used to generate equivalent atoms. #1 x,-1+y,z; #2 1-x,1-y,-z; #3 x,1+y,z; #4 1-x,-y,1-z; #5 -1+x,y,z; #6 1+x,y,z.

References

1. Zhan, C.; Ou, S.; Zou, C.; Zhao, M.; Wu, C.-D., A luminescent mixed-lanthanide-organic framework sensor for decoding different volatile organic molecules. *Anal. Chem.* **2014,** *86*, 6648-6653.

2. Wang, B.; Lv, X.-L.; Feng, D.; Xie, L.-H.; Zhang, J.; Li, M.; Xie, Y.; Li, J.-R.; Zhou, H.-C., Highly stable Zr (IV)-based metal–organic frameworks for the detection and removal of antibiotics and organic explosives in water. *J. Am. Chem. Soc.* **2016,** *138*, 6204-6216.

3. Sheldrick, G. M., Siemens area correction absorption correction program. *University of Göttingen, Göttingen, Germany* **1994**.

4. Sheldrick, G. M., SHELXL-97 program for crystal structure solution and refinement. *University of Göttingen, Göttingen, Germany* **1997**.

5. Farrugia, J. L., WinGx suite for small-molecule single crystal crystallography. *J. Appl. Crystallogr.* **1999,** *32*, 837.

6. Bourhis, L. J.; Dolomanov, O. V.; Gildea, R. J.; Howard, J. A.; Puschmann, H., The anatomy of a comprehensive constrained, restrained refinement program for the modern computing environment - Olex2 dissected. *Acta Crystallogr. A: Found. Adv.* **2015,** *71*, 59-75.

7. Dolomanov, O. V.; Bourhis, L. J.; Gildea, R. J.; Howard, J. A.; Puschmann, H., OLEX2: a complete structure solution, refinement and analysis program. *J. Appl. Crystallogr.* **2009,** *42*, 339-341.

8. Khan, S.; Markad, D.; Mandal, S. K., Two Zn (II)/Cd (II) Coordination Polymers as Recyclable Heterogeneous Catalysts for an Efficient Room-Temperature Synthesis of α-Aminonitriles via the Solvent-Free Strecker Reaction. *Inorg. Chem.* **2022,** *62*, 275-284.

9. Reinares-Fisac, D.; Aguirre-Díaz, L. M.; Iglesias, M.; Snejko, N.; Gutiérrez-Puebla, E.; Monge, M. Á.; Gándara, F., A mesoporous indium metal–organic framework: remarkable advances in catalytic activity for strecker reaction of ketones. *J. Am. Chem. Soc.* **2016,** *138*, 9089-9092.

10. Sachan, S. K.; Anantharaman, G., Cuboctahedral $[In_{36}(\mu\text{-}OH)_{24}(NO_3)_8(Imtb)_{24}]$ MOF with Atypical Pyramidal Nitrate Ion in SBU: Lewis Acid–Base Assisted Catalysis and Nanomolar Sensing of Picric Acid. *Inorg. Chem.* **2021,** *60*, 9238-9242.

11. Verma, G.; Forrest, K.; Carr, B. A.; Vardhan, H.; Ren, J.; Pham, T.; Space, B.; Kumar, S.; Ma, S., Indium–organic Framework with soc Topology as a Versatile Catalyst for Highly Efficient One-pot Strecker Synthesis of α-aminonitriles. *ACS Appl. Mater. Interfaces* **2021,** *13*, 52023-52033.

12. Verma, A.; Tomar, K.; Bharadwaj, P. K., Chiral Cadmium(II) Metal–Organic Framework from an Achiral Ligand by Spontaneous Resolution: An Efficient Heterogeneous Catalyst for the Strecker Reaction of Ketones. *Inorg. Chem.* **2017,** *56*, 13629-13633.

13. Gupta, V.; Mandal, S. K., Design and construction of a chiral Cd(II)-MOF from achiral precursors: Synthesis, crystal structure and catalytic activity toward C–C and C–N bond forming reactions. *Inorg. Chem.* **2019,** *58*, 3219-3226.

14. Gupta, V.; Mandal, S. K., A microporous metal–organic framework catalyst for solvent-free strecker reaction and CO2 fixation at ambient conditions. *Inorg. Chem.* **2020,** *59*, 4273-4281.

15. Gupta, M.; De, D.; Tomar, K.; Bharadwaj, P. K., From Zn (II)-carboxylate to double-walled Zn (II)-carboxylato phosphate MOF: change in the framework topology, capture and conversion of CO_2, and catalysis of strecker reaction. *Inorg. Chem.* **2017,** *56*, 14605-14611.

16. Karmakar, A.; Paul, A.; Santos, P. M.; Santos, I. R.; da Silva, M. F. C. G.; Pombeiro, A. J., Design and construction of polyaromatic group containing Cd (ii)-based coordination polymers for solvent-free Strecker-type cyanation of acetals. *New J. Chem.* **2022,** *46*, 10201-10212.

17. Aguirre-Díaz, L. M.; Gándara, F.; Iglesias, M.; Snejko, N.; Gutiérrez-Puebla, E.; Monge, M. Á., Tunable Catalytic Activity of Solid Solution Metal–Organic Frameworks in One-Pot Multicomponent Reactions. *J. Am. Chem. Soc.* **2015,** *137*, 6132-6135.

18. Sahoo, R.; Mondal, S.; Chand, S.; Das, M. C., Highly Robust Metal–Organic Framework for Efficiently Catalyzing Knoevenagel Condensation and the Strecker Reaction under Solvent-Free Conditions. *Inorg. Chem.* **2023,** *62*, 12989-13000.

19. Khan, S.; Markad, D.; Mandal, S. K., Two Zn(II)/Cd(II) Coordination Polymers as Recyclable Heterogeneous Catalysts for an Efficient Room-Temperature Synthesis of α-Aminonitriles via the Solvent-Free Strecker Reaction. *Inorg. Chem.* **2023,** *62*, 275-284.

20. Gandhi, S.; Sharma, V.; Koul, I. S.; Mandal, S. K., Shedding Light on the Lewis Acid Catalysis in Organic Transformations Using a Zn-MOF Microflower and Its ZnO Nanorod. *Catal. Letters* **2023,** *153*, 887-902.

21. Chai, J.; Zhang, P.; Xu, J.; Qi, H.; Sun, J.; Jing, S.; Chen, X.; Fan, Y.; Wang, L., An in-based 3D metal-organic framework as heterogeneous Lewis acid catalyst for multi-component Strecker reactions. *Inorg. Chim. Acta* **2018,** *479*, 165-171.

22. Gómez-Oliveira, E. P.; Méndez, N.; Iglesias, M.; Gutiérrez-Puebla, E.; Aguirre-Díaz, L. M.; Monge, M. Á., Building a Green, Robust, and Efficient Bi-MOF Heterogeneous Catalyst for the Strecker Reaction of Ketones. *Inorg. Chem.* **2022,** *61*, 7523-7529.

23. Rouhani, F.; Morsali, A., Highly effective Brønsted base/lewis acid cooperative catalysis: a new Cd metal–organic framework for the synthesis of Hantzsch 1, 4-DHPs at ambient temperature. *New J. Chem.* **2017,** *41*, 15475-15484.

24. Srinivasan, V. V.; Pachamuthu, M. P.; Maheswari, R., Lewis acidic mesoporous Fe-TUD-1 as catalysts for synthesis of Hantzsch 1,4-dihydropyridine derivatives. *J. Porous Mater.* **2015,** *22*, 1187-1194.

25. Maheswari, R.; Srinivasan, V. V.; Ramanathan, A.; Pachamuthu, M. P.; Rajalakshmi, R.; Imran, G., Preparation and characterization of mesostructured Zr-SBA-16: efficient Lewis acidic catalyst for Hantzsch reaction. *J. Porous Mater.* **2015,** *22*, 705-711.

26. Rostamnia, S.; Morsali, A., Basic isoreticular nanoporous metal–organic framework for Biginelli and Hantzsch coupling: IRMOF-3 as a green and recoverable heterogeneous catalyst in solvent-free conditions. *RSC Adv.* **2014,** *4*, 10514-10518.

27. Seal, N.; Neogi, S., Intrinsic-unsaturation-enriched biporous and chemorobust Cu(II) framework for efficient catalytic CO_2 fixation and pore-fitting actuated size-exclusive hantzsch condensation with mechanistic validation. *ACS Appl. Mater. Interfaces* **2021,** *13*, 55123-55135.

28. Sarkar, A.; Mondal, P. P.; Nayek, H. P., One-Pot and Solvent-Free Hantzsch Condensation Reaction Catalyzed by Mononuclear Dy (III) Complex. *ChemistrySelect* **2020,** *5*, 12302-12306.

29. Sahoo, R.; Pramanik, B.; Mondal, S.; Das, M. C., A Highly Chemically Robust 3D Interpenetrated MOF Heterogeneous Catalyst for the Synthesis of Hantzsch 1,4-Dihydropyridines and Drug Molecules. *Small* **2024**, 2309281.

30. Rostamnia, S.; Alamgholiloo, H.; Jafari, M., Ethylene diamine post-synthesis modification on open metal site Cr-MOF to access efficient bifunctional catalyst for the Hantzsch condensation reaction. *Appl. Organomet. Chem.* **2018,** *32*, e4370.

31. Ghorbani-Choghamarani, A.; Mohammadi, M.; Shiri, L.; Taherinia, Z., Synthesis and characterization of spinel $FeAl_2O_4$ (hercynite) magnetic nanoparticles and their application in multicomponent reactions. *Res. Chem. Intermed.* **2019,** *45*, 5705-5723.

32. Hajjami, M.; Gholamian, F., Tribromide ion immobilized on magnetic nanoparticle as a new, efficient and reusable nanocatalyst in multicomponent reactions. *RSC Adv.* **2016,** *6*, 87950-87960.

33. Saha, A.; Pal, A.; Mukherjee, D.; Pal, S. C.; Das, M. C., Two-Dimensional Cu (II)-MOF with Lewis Acid–Base Bifunctional Sites for Chemical Fixation of CO2 and Bioactive 1,4-DHP Synthesis via Hantzsch Condensation. *Inorg. Chem.* **2024,** *63*, 10832-10842.

34. Hajiashrafi, T.; Karimi, M.; Heydari, A.; Tehrani, A. A., Erbium-Organic Framework as Heterogeneous Lewis Acid Catalysis for Hantzsch Coupling and Tetrahydro-4H-Chromene Synthesis. *Catal. Letters* **2017,** *147*, 453-462.

35. Devarajan, N.; Suresh, P., MIL-101-SO_3H metal–organic framework as a Brønsted acid catalyst in Hantzsch reaction: an efficient and sustainable methodology for one-pot synthesis of 1,4-dihydropyridine. *New J. Chem.* **2019,** *43*, 6806-6814.

36. Aryanejad, S.; Bagherzade, G.; Moudi, M., Green synthesis and characterization of novel Mn-MOFs with catalytic and antibacterial potentials. *New J. Chem.* **2020,** *44*, 1508-1516.